PHYSICAL REVIEW B **79**, 020507(R) (2009)

Engineered selection rules for tunable coupling in a superconducting quantum circuit

K. Harrabi,[1] F. Yoshihara,[2] A. O. Niskanen,[3] Y. Nakamura,[1,2,4] and J. S. Tsai[1,2,4]
[1]*CREST-JST, Kawaguchi, Saitama 332-0012, Japan*
[2]*The Institute of Physical and Chemical Research (RIKEN), Wako, Saitama 351-0198, Japan*
[3]*VTT Technical Research Centre of Finland, Sensors, P.O. Box 1000, 02044 VTT, Espoo, Finland*
[4]*NEC Nano Electronics Research Laboratories, Tsukuba, Ibaraki 305-8501, Japan*
(Received 20 November 2008; published 20 January 2009)

Engineering selection rules of transitions is a useful strategy for coupling and decoupling qubits in superconducting quantum circuits. Following this approach, we implement a tunable coupling scheme between two flux qubits. The qubits are coupled parametrically under microwave driving via the nonlinear inductance of a third qubit. The measured on-state coupling as well as the off-state residual coupling depends on the coupler bias and agrees quantitatively with a calculation of transition matrix elements of a three-qubit Hamiltonian.

DOI: 10.1103/PhysRevB.79.020507 PACS number(s): 74.50.+r, 85.25.Cp, 03.67.−a

Superconducting qubits (see, e.g., Ref. 1 for a recent review) are among the most promising candidates for the implementation of quantum information processing. Simple demonstrations of quantum algorithms are currently within the reach of experimentalists. Nontrivial two-qubit manipulations are possible with fixed coupling between qubits.[2,3] However, for more complicated experiments with multiple qubits and future scale-up it is crucial to switch on and off the coupling energy between qubits dynamically and precisely.

There are two obvious routes toward controlling the effective interaction between qubits. One option is to control the coupling energy between qubits (actual tunable coupling).[4–9] Such schemes have been implemented by several groups and observed spectroscopically or by monitoring ground-state properties.[10–13] Expanding those ideas, a microwave approach was also developed.[14–17] This parametric driving approach has the benefit of functioning ideally at the coherence optimal point,[18–20] which is of particular importance for flux qubits that are the topic of the present study. The scheme relies on engineering two-qubit transition rules and canceling static interactions using nonlinear quantum couplers. Proposals for microwave controllable coupling without intermediate coupler elements exist as well.[21,22] These methods overcome selection rule issues either using double resonances or biasing slightly away from the optimal point. For more discussion on the selection rules in superconducting quantum circuits, see Refs. 23 and 24.

The competing approach is controlling the detuning between qubits in the presence of a small fixed off-diagonal interaction. This works nicely for two qubits,[25,26] and has been generalized by using a resonator to mediate the coupling in the spirit of cavity QED.[27–29] The main difference between these approaches is that in the tunable coupling paradigm control happens via a two-qubit operator while in the detuning approach control is solely via single-qubit terms in the system Hamiltonian. A benefit of nonlinear couplers is the possibility of suppressed off-state coupling, both in diagonal and off-diagonal, without sacrificing the on-state coupling strength.[30] For multiqubit experiments detuning alone may not suffice because the off-diagonal coupling terms persist.

In this Rapid Communication we implement a tunable coupling scheme where two flux qubits biased at the coherence optimal points are inductively coupled via a third coupler qubit.[15] We study the dc bias dependence of the tunable coupling, facilitated by the versatile on-chip coil design, and quantitatively characterize the transition matrix elements and the residual coupling energy.

The three-qubit system is described by the Hamiltonian

$$H = -\frac{1}{2}\sum_{j=1}^{3}(\Delta_j\tilde{\sigma}_z^j + \varepsilon_j\tilde{\sigma}_x^j) + \sum_{k=1}^{3}\sum_{l=k+1}^{3} J_{kl}\tilde{\sigma}_x^k\tilde{\sigma}_x^l, \qquad (1)$$

where Δ_j and $\varepsilon_j = 2I_{pj}\delta\Phi_j$ are, respectively, the tunneling and bias energies between the two persistent-current states of qubit j, and $\tilde{\sigma}_x^j$ and $\tilde{\sigma}_z^j$ are the Pauli matrices operating on qubit j. The persistent current is I_{pj}, and the flux bias with respect to the degeneracy point is $\delta\Phi_j = \Phi_j - \Phi_0/2$ where $\Phi_0 = h/(2e)$. The coupling energy is given by $J_{kl} = M_{kl}I_{pk}I_{pl}$, where M_{kl} is the mutual inductance between qubits k and l.

When qubits 1 and 2 are biased near the degeneracy points $\delta\Phi_1 \approx \delta\Phi_2 \approx 0$ and when the condition $\Delta_1 < \Delta_2 \ll \Delta_3$ is fulfilled, an adiabatic approximation on qubit 3, or the coupler, results in an effective two-qubit Hamiltonian. In order to suppress dephasing due to flux noise, we operate the qubits at the coherence optimal points where the single-qubit excitation energies of qubits 1 and 2, E_{10} and E_{01}, are insensitive to the global magnetic field. Then, the effective Hamiltonian consists of two diagonal single-qubit terms and an off-diagonal coupling term $+J_{12}^{\mathrm{eff}}\sigma_x^1\sigma_x^2$ (Ref. 15). Here we have introduced the Pauli matrices without a tilde for the effective two-qubit system. The coupling strength is given by

$$J_{12}^{\mathrm{eff}} \simeq J_{12} - \frac{2J_{23}J_{13}\Delta_3^2}{(\Delta_3^2 + \varepsilon_3^2)^{3/2}}, \qquad (2)$$

where the first and second terms can be understood, respectively, as the direct and indirect inductive interaction. If qubits 1 and 2 are far detuned, i.e., $|J_{12}^{\mathrm{eff}}| \ll |\Delta_1 - \Delta_2|$, the effect of the off-diagonal coupling becomes negligible, and the two qubits are decoupled in the first order. (See below for the discussion on further decoupling.)

To switch on the coupling, microwave modulation of $\delta\Phi_3$, with an amplitude of $\delta\Phi_3^{\mathrm{ac}}$, is applied to the coupler. Owing

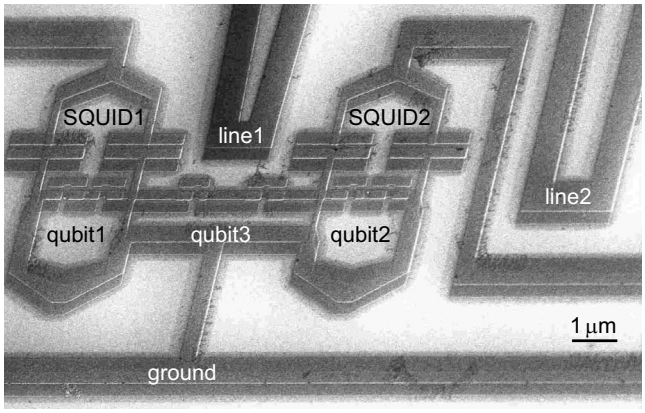

FIG. 1. Scanning electron micrograph of the three coupled flux qubits with two readout dc SQUIDs, taken from an angle. The sample was fabricated by electron-beam lithography and shadow evaporation technique using Al films. Each qubit is a superconducting loop intersected by four Josephson junctions, among which one is α_j $(j=1,2,3)$ times smaller compared to others. The α_j values (~ 0.5) are designed to satisfy the condition $\Delta_1 < \Delta_2 \ll \Delta_3$. Two qubits (qubits 1 and 2) are individually integrated into SQUIDs for the readout (SQUIDs 1 and 2). The third one (qubit 3), which is placed in between and shares a part of the loop with qubits 1 and 2, serves as a coupler. An external superconducting coil is used to apply a global magnetic flux. Together with two local bias lines (lines 1 and 2), it allows us to control the flux bias of each qubit, Φ_j, independently. The sample was placed at a temperature of about 20 mK in a dilution refrigerator.

to Eq. (2), the matrix element $\langle 00|(\partial H/\partial \Phi_3)|11\rangle$, $\langle 01|(\partial H/\partial \Phi_3)|10\rangle \simeq (\partial J_{12}^{\mathrm{eff}}/\partial \Phi_3)$ is finite. The bras and kets represent eigenstates of the effective two-qubit system. When the microwave pulse is at the sum or difference frequency of the two qubits, it parametrically induces the transition $|00\rangle \leftrightarrow |11\rangle$ or $|10\rangle \leftrightarrow |01\rangle$ and effectively switches on the coupling in the form of the operator $\sigma_x^1\sigma_x^2 \mp \sigma_y^1\sigma_y^2$ in the rotating frame. Note that though a finite J_{12}^{eff} modifies the eigenstates and renormalizes the qubit energies, due to symmetry two-qubit transitions are still forbidden in the first order for a flux drive on either qubit 1 or 2. This is why the coupler is required.

Experiments were done with the three-qubit sample shown in Fig. 1. For qubit manipulations, microwave pulses with controllable durations were applied through a current line (not shown) which was inductively coupled to all the qubits, more or less uniformly, with a mutual inductance $M \approx 0.1$ pH. The relaxation times of the two qubits were around 300 ns, limited possibly by the bias current noise flowing asymmetrically into each superconducting quantum interference device (SQUID).[20] The qubit readout was performed by using switching of the SQUIDs from the supercurrent state to the voltage state under a current pulse.[31] Change in the switching probability reflects excitation of qubits from the ground state. To avoid readout crosstalk, only one SQUID was operated at a time, and the bias current of the second one was kept at zero.

To characterize the qubits, we performed spectroscopy measurements using SQUIDs 1 and 2 individually. The qubits were excited with a microwave pulse of 5-μs duration

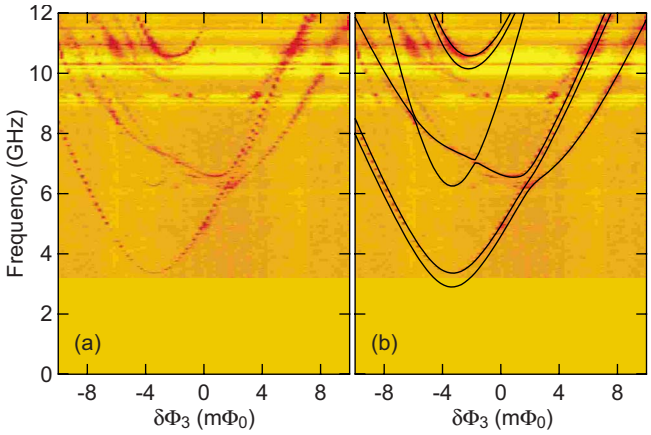

FIG. 2. (Color online) (a) Spectrum at 3.2–12 GHz of the three-qubit system measured with SQUID 2 as a function of the flux bias. The global flux bias was swept under a condition of $\delta\Phi_1 \simeq \delta\Phi_2 \simeq \delta\Phi_3 - 3$ mΦ_0. Dark (red) and bright (yellow) indicate low and high switching probabilities of the readout SQUID, respectively. The readout contrast is at best about 15%. (b) Calculated energy levels of a three-qubit Hamiltonian (solid lines) are plotted on the same data. The fitting parameters obtained from the least-squares method are as follows: $I_{p1}/h = 579 \pm 6$ GHz/Φ_0, $I_{p2}/h = 602 \pm 8$ GHz/Φ_0, $I_{p3}/h = 579 \pm 10$ GHz/Φ_0, $\Delta_1/h = 2.92 \pm 0.09$ GHz, $\Delta_2/h = 3.37 \pm 0.05$ GHz, $\Delta_3/h = 6.40 \pm 0.05$ GHz, $J_{12}/h = -0.02 \pm 0.03$ GHz, $J_{23}/h = 0.42 \pm 0.05$ GHz, $J_{13}/h = 0.44 \pm 0.04$ GHz. The unfitted traces are attributed to coupled excitations among the qubits and resonant modes in the circuit under the relatively strong microwave drive.

before each readout. Figure 2 illustrates a wide-range spectrum taken with SQUID 2. The global flux bias was swept in the measurement. Because of the geometry, signals from qubits 2 and 3 are mainly seen. The spectrum is rather complicated due to the interactions. Nevertheless, it is fitted well with the eight-level Hamiltonian (1), and all the relevant qubit parameters are deduced reliably (see also Ref. 32).

We now focus on the effective two-qubit system. In Fig. 3 we show the detailed spectroscopy as a function of $\delta\Phi_3$. While qubits 1 and 2 are kept at the coherence optimal points the single-qubit excitation energies, E_{10} and E_{01}, and the collective excitation energy, E_{11} are plotted. The $\delta\Phi_3$ dependence of the excitation energies is perfectly fitted by using the parameters in the caption of Fig. 2 after refinement within the error bars.

As a measure of the on-state coupling, we use the oscillation frequency Ω_{2q} of the $|00\rangle \leftrightarrow |11\rangle$ transition, determined by time-domain measurements. Applying a microwave pulse in resonance with this transition for the time $1/(2\Omega_{2q})$ generates a gate equivalent to the iSWAP gate, which composes a universal set of gates together with some single-qubit gates. The Rabi frequency is naturally driving-power dependent; hence, we use the maximum microwave power allowed in the measurement setup. Figure 4(a) shows Ω_{2q} as a function of $\delta\Phi_3$ while the flux biases of qubits 1 and 2 are kept at the coherence optimal points. The Rabi frequency shows nonmonotonic dependence, which is well compared to the ideal case predicted by Eq. (2): the transition matrix element $|\langle 00|(\partial H/\partial \Phi_3)|11\rangle|$ vanishes at $\delta\Phi_3 = 0$ and has a maximum

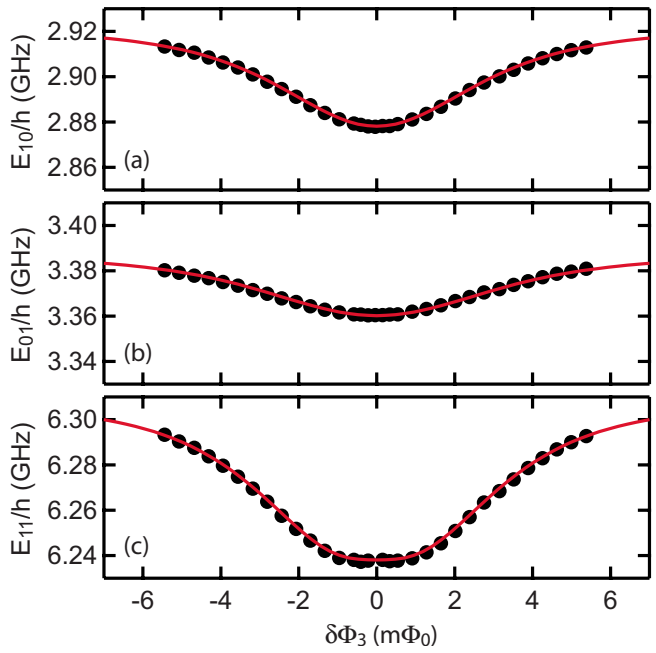

FIG. 3. (Color online) Detailed spectroscopy in the weak excitation power limit for a range of the coupler flux bias $\delta\Phi_3$. Qubits 1 and 2 are kept at their coherence optimal points. [(a),(b)] Energies of the single-qubit excitations from the ground state, E_{10} and E_{01}, measured respectively using SQUIDs 1 and 2. (c) Energy of the collective excitation of the two qubits, E_{11}. The red solid lines represent a fitting using the three-qubit Hamiltonian.

at around $|\delta\Phi_3|=\Delta_3/(4I_{p3})$. Despite the smallness of Δ_3, numerical calculation based on the three-qubit Hamiltonian further confirms quantitative agreement as depicted by the solid line in Fig. 4(a). Note that the flux drive is still in the linear regime as the drive amplitude is small compared to the peak width. The numerics also show that the contribution of simultaneous flux drives on qubits 1 and 2 is very small due to the suppressed transition matrix elements. The result remarkably demonstrates what has been predicted in theory[15] and measured before in a special case without on-chip coils,[17] i.e., proper dc biasing of the coupler qubit indeed modifies the selection rule of the sum-frequency transition. Moreover, with help of the bias coils, we can tune to the maximum of the transition matrix element.

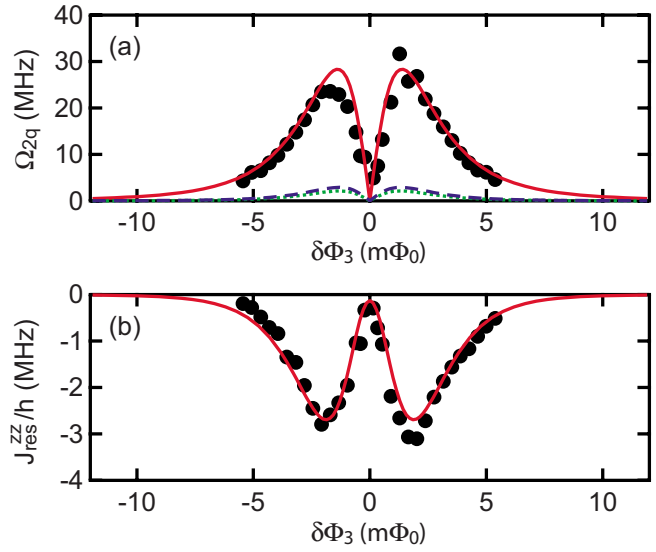

FIG. 4. (Color online) (a) Rabi frequency Ω_{2q} of the sum-frequency transition vs $\delta\Phi_3$. The solid line (red) is the calculated value $|\langle 00|(\partial H/\partial\Phi_3)|11\rangle|\delta\Phi_3^{\mathrm{ac}}/h$ assuming $\delta\Phi_3^{\mathrm{ac}}=0.52$ mΦ_0. The dashed (blue) and dotted (green) lines depict Rabi frequencies induced by the same amount of flux drive on qubits 1 and 2, respectively. (b) Residual coupling J_{res}^{zz} in the off state vs $\delta\Phi_3$. The solid line (red) is the calculated value using the three-qubit Hamiltonian.

In the absence of the microwave drive, the coupling should be ideally zero. However, the effective coupling in Eq. (2) is not exactly zero, as the compensation between the direct and indirect coupling terms is not complete. Indeed, J_{12} is supposed to be negligible in the particular sample design. Therefore, the residual off-diagonal coupling of the form $+J_{\mathrm{res}}^{xx}\sigma_x^1\sigma_x^2$ shifts E_{01} and E_{10} by $\pm(J_{\mathrm{res}}^{xx})^2/|\Delta_1-\Delta_2|$, respectively. As $|\Delta_1-\Delta_2|$ is rather small in this sample, the energy shift is relatively large. At the condition where we get the maximum Ω_{2q}, it is estimated to be ± 3.8 MHz from Eq. (2), while the integration of the red curve in Fig. 4(a) gives an estimation of ± 49 MHz, indicating that the adiabatic approximation is not very accurate due to the small Δ_3. However, in the case of two-qubit experiments, the effect can be considered merely as a renormalization of single-qubit frequencies. In a multiqubit system, on the other hand, single-qubit Rabi frequencies depend on the states of other qubits. Therefore, for perfect decoupling and unconditional single-qubit operations, one has to carefully suppress the J_{res}^{xx} term.[30]

We also find that there exists another residual coupling term in the form of $-(J_{\mathrm{res}}^{zz}/2)\sigma_z^1\sigma_z^2$. The residual coupling strength is determined by $J_{\mathrm{res}}^{zz}=(E_{11}-E_{01}-E_{10})/2$ from the data in Fig. 3 and plotted in Fig. 4(b). It shows nonmonotonic dependence on $\delta\Phi_3$, and again well reproduced by the calculation. From the comparison of Figs. 4(a) and 4(b), we see that the on/off ratio defined as $|h\Omega_{2q}/J_{\mathrm{res}}^{zz}|$ is at best ~ 10 in this sample.

In a realistic quantum processor architecture, Ω_{2q} should be as large as possible, and J_{res}^{zz} and J_{res}^{xx} should be small. Having confirmed that the three-qubit Hamiltonian (1) accurately describes the system, we can optimize the parameters for achieving a better on/off ratio. For the purpose, increase in Δ_3 is naturally preferable as it makes the adiabatic approximation better, though it tends to reduce Ω_{2q}. Nevertheless, by adjusting other parameters together, we can increase the on/off ratio without sacrificing Ω_{2q}, as the relevant quantities scale favorably with Δ_3 (Ref. 30). For example, if we choose $I_{p1}=I_{p2}=I_{p3}=600$ GHz/Φ_0, $\Delta_1/h=3$ GHz, $\Delta_2/h=5$ GHz, $\Delta_3/h=15$ GHz and $\delta\Phi_3^{\mathrm{ac}}=2$ mΦ_0, $J_{12}/h=0.049$ GHz and $J_{13}/h=J_{23}/h=0.64$ GHz are required in order to obtain the maximal on-state Rabi frequency of 10 MHz and to maximize the on/off ratio, under a constraint of $J_{\mathrm{res}}^{xx}=0$. Then, the on/off ratio can be ~ 270.

In conclusion, we have studied the parametrically-induced tunable coupling scheme between two flux qubits biased at the coherence optimal points. The on-state coupling as well as the off-state residual coupling depends nonmonotonically on the flux bias of the coupler qubit. The dependence agrees quantitatively with the calculations based on the three-qubit

Hamiltonian. The present study is an example of engineered quantum-state transition rules as well as controllable static qubit-qubit interaction. We are able to sweep the flux bias of the coupler qubit from the region of forbidden two-qubit transition to a special bias point of maximal two-qubit Rabi frequency. We expect future superconducting quantum circuits aimed at quantum information processing to generalize this idea. For instance, nonlinear couplers could be used to mediate and modulate couplings between qubits and a resonator as a quantum information bus.

We are grateful to S. Ashhab, P. Bertet, P.-M. Billangeon, and S. Lloyd for valuable discussions. A.O.N. acknowledges support from the Academy of Finland.

[1] J. Clarke and F. K. Wilhelm, Nature (London) **453**, 1031 (2008).
[2] T. Yamamoto, Yu. A. Pashkin, O. Astafiev, Y. Nakamura, and J. S. Tsai, Nature (London) **425**, 941 (2003).
[3] J. H. Plantenberg, P. C. de Groot, C. J. P. M. Harmans, and J. E. Mooij, Nature (London) **447**, 836 (2007).
[4] Yu. Makhlin, G. Schön, and A. Shnirman, Nature (London) **398**, 305 (1999).
[5] D. V. Averin and C. Bruder, Phys. Rev. Lett. **91**, 057003 (2003).
[6] B. L. T. Plourde, J. Zhang, K. B. Whaley, F. K. Wilhelm, T. L. Robertson, T. Hime, S. Linzen, P. A. Reichardt, C.-E. Wu, and J. Clarke, Phys. Rev. B **70**, 140501(R) (2004).
[7] A. Maassen van den Brink, A. J. Berkley, and M. Yalowsky, New J. Phys. **7**, 230 (2005).
[8] A. J. Kerman and W. D. Oliver, Phys. Rev. Lett. **101**, 070501 (2008).
[9] Y.-D. Wang, A. Kemp, and K. Semba, Phys. Rev. B **79**, 024502 (2009).
[10] T. Hime, P. A. Reichardt, B. L. T. Plourde, T. L. Robertson, C.-E. Wu, A. V. Ustinov, and J. Clarke, Science **314**, 1427 (2006).
[11] S. H. W. van der Ploeg, A. Izmalkov, A. M. van den Brink, U. Hübner, M. Grajcar, E. Il'ichev, H.-G. Meyer, and A. M. Zagoskin, Phys. Rev. Lett. **98**, 057004 (2007).
[12] R. Harris, A. J. Berkley, M. W. Johnson, P. Bunyk, S. Govorkov, M. C. Thom, S. Uchaikin, A. B. Wilson, J. Chung, E. Holtham, J. D. Biamonte, A. Yu. Smirnov, M. H. S. Amin, and A. Maassen van den Brink, Phys. Rev. Lett. **98**, 177001 (2007).
[13] A. Fay, E. Hoskinson, F. Lecocq, L. P. Levy, F. W. J. Hekking, W. Guichard, and O. Buisson, Phys. Rev. Lett. **100**, 187003 (2008).
[14] P. Bertet, C. J. P. M. Harmans, and J. E. Mooij, Phys. Rev. B **73**, 064512 (2006).
[15] A. O. Niskanen, Y. Nakamura, and J. S. Tsai, Phys. Rev. B **73**, 094506 (2006).
[16] M. Grajcar, Y.-X. Liu, F. Nori, and A. M. Zagoskin, Phys. Rev. B **74**, 172505 (2006).
[17] A. O. Niskanen, K. Harrabi, F. Yoshihara, Y. Nakamura, S. Lloyd, and J. S. Tsai, Science **316**, 723 (2007).
[18] D. Vion, A. Aassime, A. Cottet, P. Joyez, H. Pothier, C. Urbina, D. Esteve, and M. H. Devoret, Science **296**, 886 (2002).
[19] P. Bertet, I. Chiorescu, G. Burkard, K. Semba, C. J. P. M. Harmans, D. P. DiVincenzo, and J. E. Mooij, Phys. Rev. Lett. **95**, 257002 (2005).
[20] F. Yoshihara, K. Harrabi, A. O. Niskanen, Y. Nakamura, and J. S. Tsai, Phys. Rev. Lett. **97**, 167001 (2006).
[21] C. Rigetti, A. Blais, and M. Devoret, Phys. Rev. Lett. **94**, 240502 (2005).
[22] Y.-X. Liu, L. F. Wei, J. S. Tsai, and F. Nori, Phys. Rev. Lett. **96**, 067003 (2006).
[23] Y.-X. Liu, J. Q. You, L. F. Wei, C. P. Sun, and F. Nori, Phys. Rev. Lett. **95**, 087001 (2005).
[24] F. Deppe, M. Mariantoni, E. P. Menzel, A. Marx, S. Saito, K. Kakuyanagi, H. Tanaka, T. Meno, K. Semba, H. Takayanagi, E. Solano, and R. Gross, Nat. Phys. **4**, 686 (2008).
[25] R. McDermott, R. W. Simmonds, M. Steffen, K. B. Cooper, K. Cicak, K. D. Osborn, S. Oh, D. P. Pappas, and J. M. Martinis, Science **307**, 1299 (2005).
[26] M. Steffen, M. Ansmann, R. C. Bialczak, N. Katz, E. Lucero, R. McDermott, M. Neeley, E. M. Weig, A. N. Cleland, and J. M. Martinis, Science **313**, 1423 (2006).
[27] A. Blais, A. Maassen van den Brink, and A. M. Zagoskin, Phys. Rev. Lett. **90**, 127901 (2003).
[28] M. A. Sillanpää, J. I. Park, and R. W. Simmonds, Nature (London) **449**, 438 (2007).
[29] J. Majer, J. M. Chow, J. M. Gambetta, J. Koch, B. R. Johnson, J. A. Schreier, L. Frunzio, D. I. Schuster, A. A. Houck, A. Wallraff, A. Blais, M. H. Devoret, S. M. Girvin, and R. J. Schoelkopf, Nature (London) **449**, 443 (2007).
[30] S. Ashhab, A. O. Niskanen, K. Harrabi, Y. Nakamura, T. Picot, P. C. de Groot, C. J. P. M. Harmans, J. E. Mooij, and F. Nori, Phys. Rev. B **77**, 014510 (2008).
[31] I. Chiorescu, Y. Nakamura, C. J. P. M. Harmans, and J. E. Mooij, Science **299**, 1869 (2003).
[32] A. O. Niskanen, K. Harrabi, F. Yoshihara, Y. Nakamura, and J. S. Tsai, Phys. Rev. B **74**, 220503(R) (2006).